Mimetic Finite Difference Operators for Second-Order Tensors on Unstructured Grids

J.C. Campbell[†], J.M. Hyman[‡] and M.J. Shashkov[‡]

[†]T-7 and T-CNLS, Los Alamos National Laboratory, Los Alamos, New Mexico, 87545

[‡]T-7, Los Alamos National Laboratory, Los Alamos, New Mexico, 87545

LA-UR-01-1806

Abstract

We use the support operators method to derive discrete approximations for the gradient of a vector and divergence of a tensor on unstructured grids in two dimensions. These discrete operators satisfy discrete analogs of the integral identities of the differential operators on unstructured grids where vector functions are defined at the grid points, and tensor functions are defined as tangential projections to the zone edges, or as normal projections to the median mesh. We evaluate the accuracy of the discrete operators by determining the order of convergence of the truncation error on structured and unstructured grids, and show that the truncation error of the method is between first and second order depending on the smoothness of the grid. In a test problem on a highly nonuniform grid, we confirm that the convergence rate is between first and second order.

1 Introduction

In this paper we describe new finite difference operators for the gradient of a vector and divergence of a tensor on general grids. The discrete operators are derived using the support operator method to mimic crucial properties of the differential operators.

Many problems of practical interest involve partial differential equations (PDE's) formulated in terms of invariant, first-order differential operators such as gradient and divergence. These operators satisfy certain integral identities, which are often related to the system of PDE's being solved. The mimetic finite difference methods [1, 2, 3] use integral identities to construct discrete operators that satisfy discrete approximations of these integral identities.

To derive these mimetic finite difference methods (FDM's) that satisfy discrete approximations of these integral identities, we begin by defining a discrete approximation to a first-order operator such as divergence or gradient. This initial operator, known as the prime operator, then supports the derivation of

other discrete operators. For example if the prime operator is chosen as the divergence, then the gradient is a derived operator, and is defined as the negative adjoint of the divergence. The integral identity relating gradient and divergence is

$$\oint_{\partial V} \mathbf{v} \cdot (\mathbf{T} \cdot \mathbf{n}) dS = \int_V \nabla \mathbf{v} : \mathbf{T} dV + \int_V \mathbf{v} \cdot (\nabla \cdot \mathbf{T}) dV \tag{1}$$

where $\mathbf{T}$ is any tensor, $\mathbf{v}$ is any vector, $\mathbf{n}$ is the normal vector to surface S, and the operator : denotes the scalar product of two tensors. In the derivation a discrete version of the identity is used.

The previous papers on mimetic FDM's [1, 2, 3] have derived expressions that use, or result in, a vector. These include the gradient of a scalar and the divergence of a vector. In this paper we derive expressions that use, or result in, a second-order tensor. These are the gradient of a vector and the divergence of a tensor. Also the previous papers formulate the operators for a logically rectangular grid. Here we do not assume a logically rectangular grid, but formulate the operators so that they can be used on unstructured grids with zones of an arbitrary number of sides.

We first derive continuous expressions for the gradient and divergence in a general curvilinear coordinate system. These expressions are then used to guide us in deriving two sets of discrete operators, depending on if the divergence or gradient is the prime operator. In both cases vector functions are defined at grid points. When the gradient is the prime operator, then the tensors are defined as tangential projections to the zone edges. When the divergence is the prime operator, then the tensors are defined as normal projections to the median mesh. Then we use numerical experiments to evaluate the truncation error of the discrete operators, and calculate the convergence rate of the solution for a test problem. Both tests are done for structured and unstructured grids.

2 Gradient of a vector and divergence of a tensor in a general coordinate system

In this section we derive continuous expressions for the gradient of a vector and divergence of a tensor using a general two dimensional curvilinear coordinate system. These expressions for the continuous case will guide us in deriving the discrete expressions.

We use two coordinate systems; the standard rectangular Cartesian coordinate system, (x, y), and a general curvilinear system, (ξ, η). In the curvilinear coordinate system, shown in Fig. 1, we define the base vectors $\mathbf{t}_\xi$ and $\mathbf{t}_\eta$ tangential to the coordinate lines, and vectors $\mathbf{n}^\xi$ and $\mathbf{n}^\eta$ normal to the coordinate lines. The Cartesian components of the basis vectors are

$$\mathbf{t}_\xi = \begin{pmatrix} \dfrac{\partial x}{\partial \xi} \\ \\ \dfrac{\partial y}{\partial \xi} \end{pmatrix} \quad , \quad \mathbf{t}_\eta = \begin{pmatrix} \dfrac{\partial x}{\partial \eta} \\ \\ \dfrac{\partial y}{\partial \eta} \end{pmatrix} . \tag{2}$$

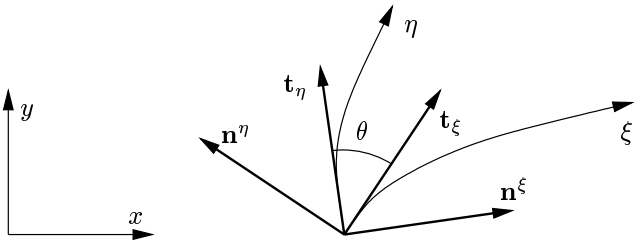

Fig. 1: The base vectors of the Cartesian (x, y) and general (ξ, η) coordinate systems. The angle θ is defined between the vectors $\mathbf{t}_\xi$ and $\mathbf{t}_\eta$ tangent to the coordinate lines. The vectors $\mathbf{n}^\xi$ and $\mathbf{n}^\eta$ are normal to $\mathbf{t}_\xi$ and $\mathbf{t}_\eta$.

$$\mathbf{n}^\xi = \begin{pmatrix} \dfrac{\partial y}{\partial \eta} \\ \\ -\dfrac{\partial x}{\partial \eta} \end{pmatrix} \quad , \quad \mathbf{n}^\eta = \begin{pmatrix} -\dfrac{\partial y}{\partial \xi} \\ \\ \dfrac{\partial x}{\partial \xi} \end{pmatrix} . \tag{3}$$

The components of the metric tensor relative to the general coordinate system are

$$g_{\xi\xi} = \mathbf{t}_\xi \cdot \mathbf{t}_\xi \quad , \quad g_{\eta\eta} = \mathbf{t}_\eta \cdot \mathbf{t}_\eta \quad , \quad g_{\xi\eta} = g_{\eta\xi} = \mathbf{t}_\eta \cdot \mathbf{t}_\xi \quad . \tag{4}$$

and its determinant is $|g| = g_{\xi\xi} g_{\eta\eta} - g_{\xi\eta} g_{\eta\xi}$.

Tensor $\mathbf{G}$ is defined as the gradient of vector $\mathbf{v}$,

$$\mathbf{G} = \nabla \mathbf{v} \tag{5}$$

which in tensor index notation is

$$G_{ij} = \frac{\partial v_i}{\partial x_j} \tag{6}$$

where $x_1 = x$, $x_2 = y$ and $\mathbf{v} = [v_1,\ v_2] = [v_x,\ v_y]$.

2.1 Tangential projections

In the general coordinate system the gradient tensor $\mathbf{G}$, or any second order tensor $\mathbf{T}$, can be represented by two column vectors which are projections to the two tangential basis vectors. These vectors are $\mathbf{G}_\xi$, $\mathbf{G}_\eta$, $\mathbf{T}_\xi$ and $\mathbf{T}_\eta$. Each vector is the dot product of the tensor with a unit base vector;

$$\mathbf{G}_\xi = \mathbf{G} \cdot \hat{\mathbf{t}}_\xi \quad , \quad \mathbf{G}_\eta = \mathbf{G} \cdot \hat{\mathbf{t}}_\eta \quad \text{and} \quad \mathbf{T}_\xi = \mathbf{T} \cdot \hat{\mathbf{t}}_\xi \quad , \quad \mathbf{T}_\eta = \mathbf{T} \cdot \hat{\mathbf{t}}_\eta \tag{7}$$

where the hat signifies a unit vector. The Cartesian components of these vectors can be written in terms of the derivatives of vector $\mathbf{v}$ with respect to ξ and η

$$\mathbf{G}_\xi = \frac{1}{\sqrt{g_{\xi\xi}}} \begin{pmatrix} \dfrac{\partial v_x}{\partial \xi} \\ \\ \dfrac{\partial v_y}{\partial \xi} \end{pmatrix} = \begin{pmatrix} \mathbf{G}_{\xi x} \\ \\ \mathbf{G}_{\xi y} \end{pmatrix} \quad , \quad \mathbf{G}_\eta = \frac{1}{\sqrt{g_{\eta\eta}}} \begin{pmatrix} \dfrac{\partial v_x}{\partial \eta} \\ \\ \dfrac{\partial v_y}{\partial \eta} \end{pmatrix} = \begin{pmatrix} \mathbf{G}_{\eta x} \\ \\ \mathbf{G}_{\eta y} \end{pmatrix} . \quad (8)$$

When using the tangential projections to represent the tensors, it is most convenient in the discrete case to define the gradient and then derive the divergence. The divergence can be expressed in terms of tangential projections of a tensor using the integral identity

$$\int_V \nabla \mathbf{v} : \mathbf{T} dV = \oint_{\partial V} \mathbf{v} \cdot (\mathbf{T} \cdot \mathbf{n}) dS - \int_V \mathbf{v} \cdot (\nabla \cdot \mathbf{T}) dV. \quad (9)$$

To use this identity to derive the divergence requires an expression for the scalar product, $\mathbf{G} : \mathbf{T}$, in terms of the tangential projections. The scalar product is defined in terms of the Cartesian components of the two tensors, so we start by defining the Cartesian components of $\mathbf{G}$ in terms of $\mathbf{G}_\xi$ and $\mathbf{G}_\eta$. These formulae are valid for any tensor, and are found by solving the set of equations represented by equation (7)

$$\begin{aligned} G_{xx} &= \frac{\partial y}{\partial \eta} \mathbf{G}_{\xi x} \sqrt{\frac{g_{\xi\xi}}{|g|}} - \frac{\partial y}{\partial \xi} \mathbf{G}_{\eta x} \sqrt{\frac{g_{\eta\eta}}{|g|}} \\ G_{xy} &= \frac{\partial x}{\partial \xi} \mathbf{G}_{\eta x} \sqrt{\frac{g_{\eta\eta}}{|g|}} - \frac{\partial x}{\partial \eta} \mathbf{G}_{\xi x} \sqrt{\frac{g_{\xi\xi}}{|g|}} \\ G_{yx} &= \frac{\partial y}{\partial \eta} \mathbf{G}_{\xi y} \sqrt{\frac{g_{\xi\xi}}{|g|}} - \frac{\partial y}{\partial \xi} \mathbf{G}_{\eta y} \sqrt{\frac{g_{\eta\eta}}{|g|}} \\ G_{yy} &= \frac{\partial x}{\partial \xi} \mathbf{G}_{\eta y} \sqrt{\frac{g_{\eta\eta}}{|g|}} - \frac{\partial x}{\partial \eta} \mathbf{G}_{\xi y} \sqrt{\frac{g_{\xi\xi}}{|g|}} . \end{aligned} \quad (10)$$

An expression for the tensor scalar product is then found by substituting these expressions into the definition of the scalar product, and collecting terms

$$\begin{aligned} \mathbf{G} : \mathbf{T} &= G_{xx} T_{xx} + G_{xy} T_{xy} + G_{yx} T_{yx} + G_{yy} T_{yy} \\ &= \mathbf{G}_\xi \cdot \left[\mathbf{T}_\xi \frac{g_{\xi\xi} g_{\eta\eta}}{|g|} - \mathbf{T}_\eta \frac{g_{\xi\eta}}{|g|} \sqrt{g_{\xi\xi} g_{\eta\eta}} \right] + \\ &\quad \mathbf{G}_\eta \cdot \left[\mathbf{T}_\eta \frac{g_{\xi\xi} g_{\eta\eta}}{|g|} - \mathbf{T}_\xi \frac{g_{\xi\eta}}{|g|} \sqrt{g_{\xi\xi} g_{\eta\eta}} \right] . \end{aligned} \quad (11)$$

Rearranging and noting that

$$\frac{g_{\xi\xi} g_{\eta\eta}}{|g|} = \frac{1}{\sin^2 \theta} \quad , \quad \frac{g_{\xi\eta}}{\sqrt{g_{\xi\xi} g_{\eta\eta}}} = \cos \theta \quad (12)$$

allows the scalar product to be written only in terms of the tangential projections and the angle θ between $\mathbf{t}_\xi$ and $\mathbf{t}_\eta$ (see Fig 1);

$$\mathbf{G} : \mathbf{T} \quad = \quad \frac{1}{\sin^2\theta}\Big[\mathbf{G}_\xi \cdot \mathbf{T}_\xi + \mathbf{G}_\eta \cdot \mathbf{T}_\eta - \cos\theta(\mathbf{G}_\xi \cdot \mathbf{T}_\eta + \mathbf{G}_\eta \cdot \mathbf{T}_\xi)\Big]. \quad (13)$$

Comparing (13) to the expression for the vector dot product in [2] shows that the two expressions are equivalent except that now the ξ and η terms are vectors instead of scalars.

In deriving an expression for the divergence using the identity in (9) we assume, for simplicity, that the surface integral is zero and use equation (13) for $\nabla\mathbf{v} : \mathbf{T}$. We then replace the $\mathbf{G}_\xi$ and $\mathbf{G}_\eta$ terms with the derivatives of vector $\mathbf{v}$ using (8) to give

$$\begin{aligned}\iint \nabla\mathbf{v} : \mathbf{T}\sqrt{|g|}d\xi d\eta \quad &= \iint \left(\frac{\partial \mathbf{v}}{\partial \xi} \cdot \left[\frac{\mathbf{T}_\xi - \cos\theta \mathbf{T}_\eta}{\sqrt{g_{\xi\xi}}\sin^2\theta} \right] + \right. \\ &\left. \frac{\partial \mathbf{v}}{\partial \eta} \cdot \left[\frac{\mathbf{T}_\eta - \cos\theta \mathbf{T}_\xi}{\sqrt{g_{\eta\eta}}\sin^2\theta} \right] \right) \sqrt{|g|}d\xi d\eta \ . \quad (14)\end{aligned}$$

Integrating this expression by parts gives two terms that are equivalent to the right hand side of equation (9). Setting the terms representing the surface integral equal to zero leaves

$$\begin{aligned}\iint \mathbf{v} \cdot (\nabla \cdot \mathbf{T})\sqrt{|g|}d\xi d\eta \quad &= \iint \left(\mathbf{v} \cdot \frac{\partial}{\partial \xi} \left[\sqrt{\frac{|g|}{g_{\xi\xi}}} \ \frac{\mathbf{T}_\xi - \cos\theta \mathbf{T}_\eta}{\sin^2\theta} \right] + \right. \\ &\left. \mathbf{v} \cdot \frac{\partial}{\partial \eta} \left[\sqrt{\frac{|g|}{g_{\eta\eta}}} \ \frac{\mathbf{T}_\eta - \cos\theta \mathbf{T}_\xi}{\sin^2\theta} \right] \right) d\xi d\eta \quad (15)\end{aligned}$$

As this expression is true for any vector $\mathbf{v}$, as we shrink the volume to zero we can define the divergence as

$$\begin{aligned}\nabla \cdot \mathbf{T} \quad &= \frac{1}{\sqrt{|g|}} \left\{ \frac{\partial}{\partial \xi} \left[\sqrt{\frac{|g|}{g_{\xi\xi}}} \ \frac{\mathbf{T}_\xi - \cos\theta \mathbf{T}_\eta}{\sin^2\theta} \right] + \right. \\ &\left. \frac{\partial}{\partial \eta} \left[\sqrt{\frac{|g|}{g_{\eta\eta}}} \ \frac{\mathbf{T}_\eta - \cos\theta \mathbf{T}_\xi}{\sin^2\theta} \right] \right\}. \quad (16)\end{aligned}$$

This definition can also be derived directly from the expression for the divergence in terms of T_{xx}, T_{yy}, T_{xy} and T_{yx}. However from a methodological point of view it is useful to derive it using the integral identity.

2.2 Normal projections

Tensors can also be expressed as the dot product of the tensor with the unit vectors normal to the coordinate axes (Fig 1);

$$\mathbf{G}^\xi = \mathbf{G} \cdot \hat{\mathbf{n}}^\xi \quad , \quad \mathbf{G}^\eta = \mathbf{G} \cdot \hat{\mathbf{n}}^\eta \quad \text{and} \quad \mathbf{T}^\xi = \mathbf{T} \cdot \hat{\mathbf{n}}^\xi \quad , \quad \mathbf{T}^\eta = \mathbf{T} \cdot \hat{\mathbf{n}}^\eta. \quad (17)$$

Note that we are using the superscript notation for the tensors expressed in terms of the vectors normal to the coordinate axis to distinguish them from tensors expressed in terms of tangential projections.

These equations can be solved to obtain

$$\begin{aligned} G_{xx} &= \frac{\partial x}{\partial \xi}\mathbf{G}^{\xi x}\sqrt{\frac{g_{\eta\eta}}{|g|}} + \frac{\partial x}{\partial \eta}\mathbf{G}^{\eta x}\sqrt{\frac{g_{\xi\xi}}{|g|}} \\ G_{xy} &= \frac{\partial y}{\partial \eta}\mathbf{G}^{\eta x}\sqrt{\frac{g_{\xi\xi}}{|g|}} + \frac{\partial y}{\partial \xi}\mathbf{G}^{\xi x}\sqrt{\frac{g_{\eta\eta}}{|g|}} \\ G_{yx} &= \frac{\partial x}{\partial \xi}\mathbf{G}^{\xi y}\sqrt{\frac{g_{\eta\eta}}{|g|}} + \frac{\partial x}{\partial \eta}\mathbf{G}^{\eta y}\sqrt{\frac{g_{\xi\xi}}{|g|}} \\ G_{yy} &= \frac{\partial y}{\partial \eta}\mathbf{G}^{\eta y}\sqrt{\frac{g_{\xi\xi}}{|g|}} + \frac{\partial y}{\partial \xi}\mathbf{G}^{\xi y}\sqrt{\frac{g_{\eta\eta}}{|g|}} \ . \end{aligned} \tag{18}$$

Following the same method used for the tangential projections gives an expression for the scalar product

$$\mathbf{G} : \mathbf{T} = \frac{1}{\sin^2\theta}\left[\mathbf{G}^{\xi}\cdot\mathbf{T}^{\xi} + \mathbf{G}^{\eta}\cdot\mathbf{T}^{\eta} + \cos\theta(\mathbf{G}^{\xi}\cdot\mathbf{T}^{\eta} + \mathbf{G}^{\eta}\cdot\mathbf{T}^{\xi})\right]. \tag{19}$$

When using normal projections it is most convenient to start with the divergence and then derive the gradient. The divergence in terms of the normal projections is derived by substituting (18) into the the definition of divergence in Cartesian components. This gives

$$\nabla\cdot\mathbf{T} = \frac{1}{\sqrt{|g|}}\left\{\frac{\partial}{\partial\xi}\left[\mathbf{T}^{\xi}\sqrt{g_{\eta\eta}}\right] + \frac{\partial}{\partial\eta}\left[\mathbf{T}^{\eta}\sqrt{g_{\xi\xi}}\right]\right\}. \tag{20}$$

We derive the gradient by substituting (20) into the integral identity (9) and eliminating the terms representing the zero surface integral to give

$$\nabla\mathbf{v} : \mathbf{T} = \frac{1}{\sqrt{|g|}}\left\{\frac{\partial\mathbf{v}}{\partial\xi}\mathbf{T}^{\xi}\sqrt{g_{\eta\eta}} + \frac{\partial\mathbf{v}}{\partial\eta}\mathbf{T}^{\eta}\sqrt{g_{\xi\xi}}\right\}. \tag{21}$$

Equating (21) with (19) allows the gradient to be written in terms of $\mathbf{G}^{\xi}$ and $\mathbf{G}^{\eta}$

$$\begin{aligned} \frac{\partial\mathbf{v}}{\partial\xi} &= \sqrt{\frac{|g|}{g_{\eta\eta}}}\ \frac{\mathbf{G}^{\xi} + \cos\theta\mathbf{G}^{\eta}}{\sin^2\theta} \\ \frac{\partial\mathbf{v}}{\partial\eta} &= \sqrt{\frac{|g|}{g_{\xi\xi}}}\ \frac{\mathbf{G}^{\eta} + \cos\theta\mathbf{G}^{\xi}}{\sin^2\theta}\ . \end{aligned} \tag{22}$$

Solving these equations for $\mathbf{G}^{\xi}$ and $\mathbf{G}^{\eta}$ in terms of the directional derivatives of the velocity results in definitions of the gradient vectors as

$$\begin{aligned} \mathbf{G}^{\xi} &= \frac{1}{\sqrt{|g|}}\left\{\frac{\partial\mathbf{v}}{\partial\xi}\sqrt{g_{\eta\eta}} - \frac{\partial\mathbf{v}}{\partial\eta}\sqrt{g_{\xi\xi}}\cos\theta\right\} \\ \mathbf{G}^{\eta} &= \frac{1}{\sqrt{|g|}}\left\{\frac{\partial\mathbf{v}}{\partial\eta}\sqrt{g_{\xi\xi}} - \frac{\partial\mathbf{v}}{\partial\xi}\sqrt{g_{\eta\eta}}\cos\theta\right\}. \end{aligned} \tag{23}$$

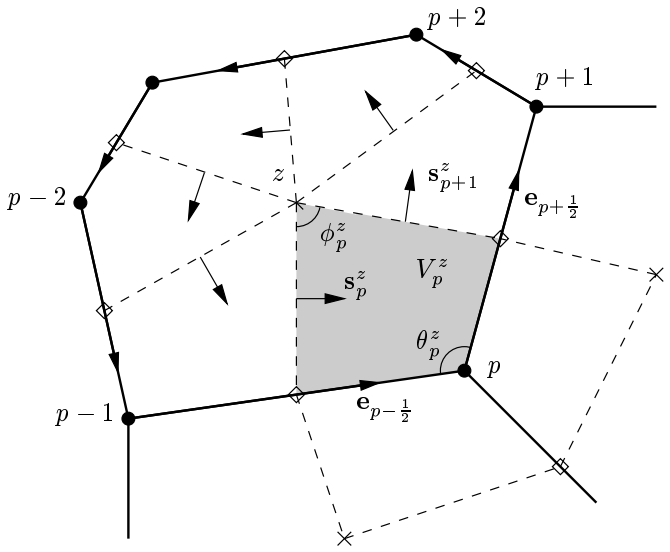

Fig. 2: Diagram of a computational zone within an unstructured staggered grid, showing zone z and point p. The solid lines define the grid, and the dashed lines show the median mesh. The median mesh is formed by connecting the zone centers, $\times$, to the mid-side points, $\diamond$. The shaded area shows a subzonal corner volume. The $\mathbf{e}$ vectors are tangential to the zone edges, and the $\mathbf{s}$ vectors are normal to the median mesh. The notation shown is relative to the selected point p.

3 Discrete Operators

This section describes the derivation of discrete expressions for the gradient of a vector and divergence of a tensor on a grid. In the support operator method a discrete approximation for a differential operator, such as divergence or gradient, is chosen. This initial or prime operator then supports the derivation of other mimetic discrete operators.

3.1 Grid

We construct the discrete functions on a spatially staggered grid. Figure 2 shows a computational zone of a unstructured staggered grid. The median mesh is constructed by connecting the zone centers with the mid-side points. The intersection of the median mesh with the grid lines gives subzonal corner volumes, one is shown as the shaded area. We denote the volume of the corner as V^z_p, where the indices denote the zone and point with which it is associated. We define $V^z_p = V^p_z$ and follow the convention of always summing with respect to the lower index. The corner volume can then be used to define both a zone

volume and a point volume.

$$V_z = \sum_{p \in S(z)} V_p^z \quad , \quad V_p = \sum_{z \in S(p)} V_z^p, \tag{24}$$

where the sums are over the stencil associated with the zone or point. The stencil for a zone is each point that is a vertex of the zone. For a point the stencil is every adjacent zone. The same super and subscript notation is used for any value that is associated with both a point and a zone.

Figure 2 also shows the notation used for the discrete operators. The notation is all relative to point p, which is a vertex of zone z. The unit vector $\hat{\mathbf{e}}_{p+\frac{1}{2}}$ is defined at the center of edge $p+\frac{1}{2}$, which connects points p and $p+1$; $l_{p+\frac{1}{2}}$ is the length of this edge. The arrows on the edges define the positive direction of $\mathbf{e}$ when considering zone z. The $\mathbf{s}$ vectors are normal to the median mesh, and have length equal to the segment of median mesh with which they are associated. The angle θ_p^z is between the two edges of zone z that meet at point p. The angle ϕ_p^z is between the two segments of median mesh which define the corner volume V_p^z.

We will derive discrete operators for the case when vector functions are defined at the grid points. The tensor functions are defined at different grid locations, depending on the choice of prime operator. We will use the gradient as prime operator when the tensor functions are represented as tangential projections to the zone edges. We use the divergence as the prime operator when the tensor functions are represented as normal projections to the median mesh. In the derivation of these operators we do not assume a structured grid, so the resulting expressions are equally applicable to structured and unstructured grids.

3.2 Tensor functions defined as tangential projections to the zone edges

3.2.1 The prime operator

When the tensors are defined as the tangential projections to the zone edges then we choose the discrete vector gradient, **GRAD**, as the prime operator.

For a direction l, given by unit vector $\hat{\mathbf{l}}$, the directional derivative of vector field $\mathbf{v}$ is:

$$\frac{\partial \mathbf{v}}{\partial l} = \hat{\mathbf{l}} \cdot \nabla \mathbf{v} \ . \tag{25}$$

This leads to the second-order approximation of the projections of tensor $\mathbf{G} =$ **GRAD** $\mathbf{v}$ as

$$\mathbf{G}^e_{p+\frac{1}{2}} = \mathbf{G}_{p+\frac{1}{2}} \cdot \hat{\mathbf{e}}_{p+\frac{1}{2}} = \frac{\mathbf{v}_{p+1} - \mathbf{v}_p}{l_{p+\frac{1}{2}}}, \tag{26}$$

where $\hat{\mathbf{e}}$ is the unit vector along the zone edge, as shown in Fig. 2. The agreement between equations (26) and (8) is clear when we recall the identities

$$dl_\xi = \sqrt{g_{\xi\xi}} d\xi \quad , \quad dl_\eta = \sqrt{g_{\eta\eta}} d\eta \tag{27}$$

where dl_ξ and dl_η are the elements of arcs of coordinate curves.

3.2.2 The derived operator

We now use the prime operator to derive the discrete divergence, **DIV**, as the negative adjoint of **GRAD**.

The first step is to derive a discrete form of equation (13), the tensor scalar product. We approximate this continuous equation by

$$(\mathbf{G}:\mathbf{T})_z = \sum_{p\in S(z)} \frac{W_p^z}{\sin^2\theta_p^z} \quad \Big\{ \mathbf{G}^e_{p-\frac{1}{2}}\cdot\mathbf{T}^e_{p-\frac{1}{2}} + \mathbf{G}^e_{p+\frac{1}{2}}\cdot\mathbf{T}^e_{p+\frac{1}{2}} + \cos\theta_p^z\left[\mathbf{G}^e_{p-\frac{1}{2}}\cdot\mathbf{T}^e_{p+\frac{1}{2}} + \mathbf{G}^e_{p+\frac{1}{2}}\cdot\mathbf{T}^e_{p-\frac{1}{2}}\right]\Big\} \tag{28}$$

which gives the scalar product evaluated in zone z, shown in Fig. 2. In this expression the sign of the cosine has changed, this is due to the sign convention adopted. The weights W_p^z satisfy the consistency conditions

$$W_p^z \geq 0 \quad , \quad \sum_{p\in S(z)} W_p^z = 1. \tag{29}$$

We define W_p^z as one half the area of the triangle in zone z which contains the angle at point p, divided by the sum of all such area in the zone. This division ensures that the weights satisfy the second condition and results in a first order approximation of the operator [4],

$$W_p^z = \frac{\frac{1}{4}l_{p+\frac{1}{2}}l_{p-\frac{1}{2}}|\sin\theta_p^z|}{\sum_{p\in S(z)}\frac{1}{4}l_{p+\frac{1}{2}}l_{p-\frac{1}{2}}|\sin\theta_p^z|}. \tag{30}$$

To derive **DIV** from (28) and (26) we use the discrete form of the integral identity (9) and, for simplicity, assume that the surface integral is zero. This gives us

$$\sum_z (\mathbf{G}:\mathbf{T})_z V_z = -\sum_p (\mathbf{v}\cdot\mathbf{DIV}\ \mathbf{T})_p V_p. \tag{31}$$

Substituting (28) into (31), and substituting for $\mathbf{G}^e$ using (26) gives an expression which contains the velocity vector at three points: $\mathbf{v}_{p+1}$, $\mathbf{v}_p$ and $\mathbf{v}_{p-1}$. Rewriting the expression by collecting all the $\mathbf{v}$ terms at point p gives

$$\begin{aligned} -\sum_p (\mathbf{v}\cdot\mathbf{DIV}\ \mathbf{T})_p V_p \;=\; & \sum_z \sum_{p\in S(z)} \mathbf{v}_p \cdot \Bigg(\\ & \frac{W_p^z}{\sin^2\theta_p^z}\left\{\frac{\mathbf{T}^e_{p-\frac{1}{2}}}{l_{p-\frac{1}{2}}} - \frac{\mathbf{T}^e_{p+\frac{1}{2}}}{l_{p+\frac{1}{2}}} + \cos\theta_p^z\left[\frac{\mathbf{T}^e_{p+\frac{1}{2}}}{l_{p-\frac{1}{2}}} - \frac{\mathbf{T}^e_{p-\frac{1}{2}}}{l_{p+\frac{1}{2}}}\right]\right\} \\ & + \frac{W_{p-1}^z}{\sin^2\theta_{p-1}^z}\left\{\frac{\mathbf{T}^e_{p-\frac{1}{2}}}{l_{p-\frac{1}{2}}} + \cos\theta_{p-1}^z\frac{\mathbf{T}^e_{p-\frac{3}{2}}}{l_{p-\frac{1}{2}}}\right\} \\ & - \frac{W_{p+1}^z}{\sin^2\theta_{p+1}^z}\left\{\frac{\mathbf{T}^e_{p+\frac{1}{2}}}{l_{p+\frac{1}{2}}} + \cos\theta_{p+1}^z\frac{\mathbf{T}^e_{p+\frac{3}{2}}}{l_{p+\frac{1}{2}}}\right\}\Bigg) V_z. \end{aligned} \tag{32}$$

The expression for **DIV T** at the grid point p can now be written as

$$
\begin{aligned}
(\mathbf{DIV\ T})_p \quad = \frac{1}{V_p} \sum_{z \in S(p)} V_z \Bigg[& \frac{1}{l_{p+\frac{1}{2}}} \left\{ \frac{W_z^{p+1}}{\sin^2 \theta_z^{p+1}} \left(\mathbf{T}^e_{p+\frac{1}{2}} + \cos\theta_z^{p+1} \mathbf{T}^e_{p+\frac{3}{2}} \right) \right\} \\
& + \frac{1}{l_{p+\frac{1}{2}}} \left\{ \frac{W_z^{p}}{\sin^2 \theta_z^{p}} \left(\mathbf{T}^e_{p+\frac{1}{2}} + \cos\theta_z^{p} \mathbf{T}^e_{p-\frac{1}{2}} \right) \right\} \\
& - \frac{1}{l_{p-\frac{1}{2}}} \left\{ \frac{W_z^{p}}{\sin^2 \theta_z^{p}} \left(\mathbf{T}^e_{p-\frac{1}{2}} + \cos\theta_z^{p} \mathbf{T}^e_{p+\frac{1}{2}} \right) \right\} \\
& - \frac{1}{l_{p-\frac{1}{2}}} \left\{ \frac{W_z^{p-1}}{\sin^2 \theta_z^{p-1}} \left(\mathbf{T}^e_{p-\frac{1}{2}} + \cos\theta_z^{p-1} \mathbf{T}^e_{p-\frac{3}{2}} \right) \right\} \Bigg].
\end{aligned} \tag{33}
$$

3.3 Tensor functions defined as normal projections to the median mesh

Now we derive expressions where the tensors are defined as normal projections to the median mesh,

$$\mathbf{T}_p^z = \mathbf{T} \cdot \hat{\mathbf{s}}_p^z \tag{34}$$

where $\hat{\mathbf{s}}_p^z$ is the unit normal vector to the median mesh, as shown in Fig. 2.

3.3.1 The prime operator

In this case, we choose the prime operator to be the divergence of a tensor $\mathbf{T}$ calculated at the grid points. The divergence is approximated as the surface integral around the median mesh surrounding a point of the normal component of the tensor.

$$(\mathbf{DIV\ T})_p = \frac{1}{V_p} \sum_{z \in S(p)} \left(\mathbf{T}^z_{p+1} |\mathbf{s}|^z_{p+1} - \mathbf{T}^z_p |\mathbf{s}|^z_p \right) \tag{35}$$

where $|\mathbf{s}|$ means the length of vector $\mathbf{s}$.

3.3.2 The derived operator

We now use the prime operator to derive the discrete gradient, **GRAD**, as the negative adjoint of **DIV**. The scalar product $(\mathbf{v}, \mathbf{DIV\ T})_p$ in (31) is defined using (35), and is used to derive an expression for the scalar product of the gradient tensor $\mathbf{G}$ with tensor $\mathbf{T}$ in a zone as

$$(\mathbf{G} : \mathbf{T})_z = \frac{1}{V_z} \sum_{p \in S(z)} \mathbf{T}^z_p \cdot (\mathbf{v}_p |\mathbf{s}|^z_p - \mathbf{v}_{p-1} |\mathbf{s}|^z_p). \tag{36}$$

To define the vector projections of the gradient tensor we define the expression for the scalar product of two tensors in a zone, using a discrete approxima-

tion of equation (19),

$$(\mathbf{G}:\mathbf{T})_z = \sum_{p\in S(z)} \frac{W_p^z}{\sin^2\phi_p^z} \quad \left\{\mathbf{G}_{p+1}^z\cdot\mathbf{T}_{p+1}^z + \mathbf{G}_p^z\cdot\mathbf{T}_p^z \right. \\ \left. -\cos\phi_p^z\left[\mathbf{G}_{p+1}^z\cdot\mathbf{T}_p^z + \mathbf{G}_p^z\cdot\mathbf{T}_{p+1}^z\right]\right\}. \tag{37}$$

Here the weights W_p^z are twice the area of the triangle in zone z formed by the two sections of the median mesh that define the corner volume, normalized by the sum of all such volumes in zone z

Equation (37) is rearranged to give

$$(\mathbf{G}:\mathbf{T})_z = \sum_{p\in S(z)} \mathbf{T}_p^z\cdot \quad \left(\frac{W_p^z}{\sin^2\phi_p^z}(\mathbf{G}_p^z - \cos\phi_p^z\mathbf{G}_{p+1}^z)\right. \\ \left. +\frac{W_{p-1}^z}{\sin^2\phi_{p-1}^z}(\mathbf{G}_p^z - \cos\phi_{p-1}^z\mathbf{G}_{p-1}^z)\right). \tag{38}$$

Equating (36) with (38) cancels the $\mathbf{T}_z^p$ terms, leaving

$$\sum_{p\in S(z)} \frac{|\mathbf{s}|_p^z}{V_z}(\mathbf{v}_p - \mathbf{v}_{p-1}) = \sum_{p\in S(z)} \left[\mathbf{G}_p^z\left(\frac{W_p^z}{\sin^2\phi_p^z} + \frac{W_{p-1}^z}{\sin^2\phi_{p-1}^z}\right)\right. \\ \left. -\mathbf{G}_{p+1}^z\left(\frac{W_p^z\cos\phi_p^z}{\sin^2\phi_p^z}\right) - \mathbf{G}_{p-1}^z\left(\frac{W_{p-1}^z\cos\phi_{p-1}^z}{\sin^2\phi_{p-1}^z}\right)\right]. \tag{39}$$

This expression allows us to solve for the $\mathbf{G}$ terms within a zone by setting up a system of n equations with n unknowns, where n is the number of sides of the zone. The x and y components of the vectors are solved for separately. Note that the main $n \times n$ matrix is the same in both cases. This main matrix is symmetric positive definite, so there are computationally fast techniques, such as Cholesky decomposition, that be used to solve the system.

3.4 Vector Laplacian

In both the tangential and normal projection cases the individual divergence and gradient operators can be combined to give a vector Laplacian operator that is a discrete approximation to

$$\nabla^2\mathbf{v} = \nabla\cdot(\nabla\mathbf{v}). \tag{40}$$

As the discrete divergence is the negative adjoint of the discrete gradient, the discrete approximation of (40) is guaranteed to be self adjoint and nonnegative definite on arbitrary grids.

Figure 3 shows the stencils for the Laplacian on meshes formed from squares, equilateral triangles and regular hexagons. For the meshes formed from squares and triangles both versions reduce to the standard second-order stencils. On

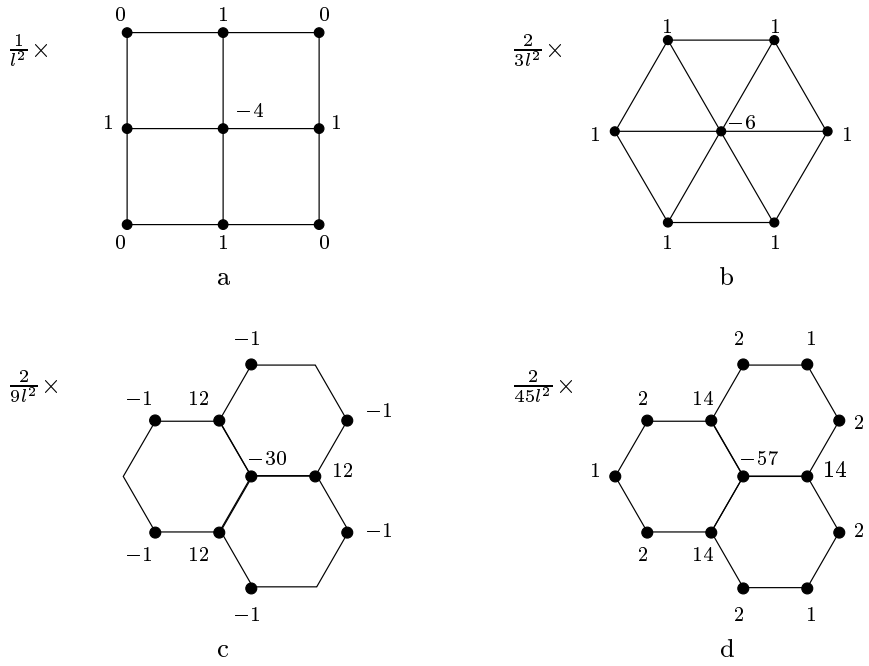

Fig. 3: The dots represent the stencil for the vector Laplacian. The coefficients define the FDM on regular grids, where l is the edge length: (a) On a square grid both approaches give the standard second order five point FDM. (b) On grid of equilateral triangles both approached give the standard second order FDM. (c) Tangential projection operator on a grid of regular hexagons. (d) Normal projection operator on a grid of regular hexagons.

the square grid the four points with a coefficient of 0 are points where the coefficient contains a $\cos\theta$ term. These points only contribute to the discrete Laplacian when the grid is not orthogonal. For the hexagonal grid the different prime operators give different stencils for the Laplacian. The Laplacian operator formed from the tangential projection divergence and gradient has a stencil including only neighbor and neighbor of neighbor points, so not every vertex of the adjacent zones is included. The operator formed from the normal projection divergence and gradient includes all vertices of the adjacent zones.

4 Numerical tests

In the first set of numerical experiments we evaluate the convergence rate of the truncation error for the individual gradient and divergence operators on structured and unstructured grids. We then check the convergence rate of the solution to Poisson's equation with Dirichlet boundary conditions.

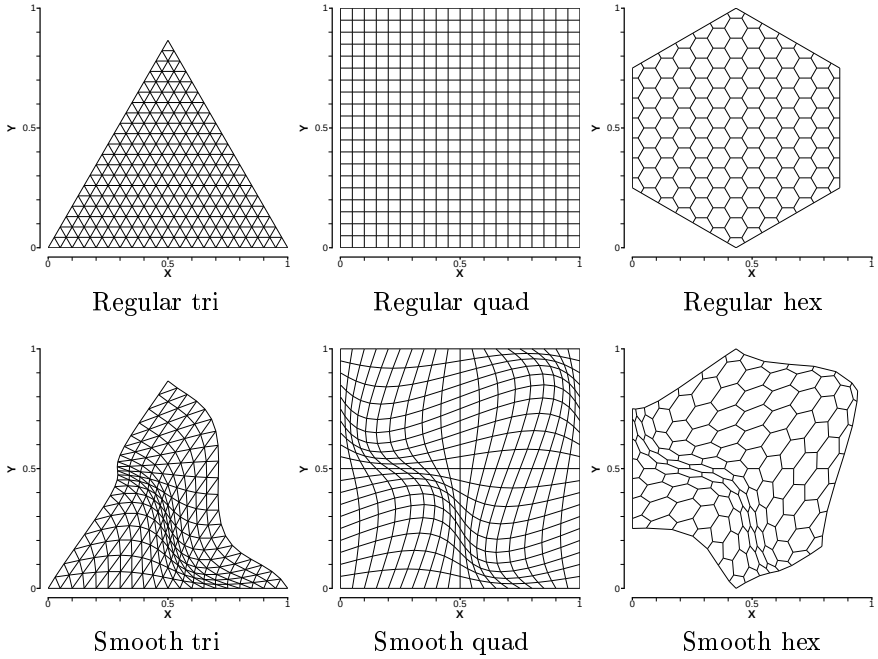

Fig. 4: The 6 grids used in the numerical tests.

The numerical experiments were performed for six progressively refined grids. Figure 4 shows the six grids at their coarsest state where the logically rectangular grids have 20×20 zones. The smooth grids are generated from the regular grids by applying the transformation

$$x' = x + 0.1\sin(2\pi x)\sin(2\pi y) \quad , \quad y' = y + 0.1\sin(2\pi x)\sin(2\pi y) \qquad (41)$$

where x and y are the original point coordinates, x' and y' are the transformed coordinates.

As the operators are formulated for arbitrary unstructured grids, the same computer code can be used for all six grids without modification.

4.1 Truncation error

To calculate the truncation error between the exact solution and the numerical approximation for a vector, we calculate the error at the grid points. For a tensor we calculate the error in its projection to either the zone edge or median mesh.

The truncation error is measured the vector and tensor functions that are

either linear or quadratic polynomials of x and y;

Linear function :

$$\mathbf{v} = [x, y] \qquad \nabla\mathbf{v} = \begin{bmatrix} 1 & 0 \\ 0 & 1 \end{bmatrix}$$

$$\mathbf{T} = \begin{bmatrix} x & 0 \\ 0 & y \end{bmatrix} \qquad \nabla \cdot \mathbf{T} = [1, 1]$$

Quadratic function :

$$\mathbf{v} = [x^2 + xy + y^2, x^2 + xy + y^2] \qquad \nabla\mathbf{v} = \begin{bmatrix} 2x + y & x + 2y \\ 2x + y & x + 2y \end{bmatrix}$$

$$\mathbf{T} = \begin{bmatrix} x^2 + xy + y^2 & x^2 + xy + y^2 \\ x^2 + xy + y^2 & x^2 + xy + y^2 \end{bmatrix} \quad \nabla \cdot \mathbf{T} = [3x + 3y, 3x + 3y]$$

The vector $\mathbf{v}$ is calculated at the grid points. For tensor $\mathbf{T}$ the coordinates of the zone or median mesh edges have to be defined. For $\mathbf{T}$ defined as a tangential projection to the zone edge, the tensor is evaluated at the mid-point of each edge, the coordinates of the mid-point are the average of the coordinates of the two end points of the edge. For $\mathbf{T}$ defined as normal projections to the median mesh, the coordinates of the mid-point of the associated edge is used to evaluate the tensor. The same locations on the grid are used when evaluating the divergence and gradient operators.

To estimate the truncation error we represent the error E_h by

$$||E_h|| = Ch^q + O(h^{q+1}) \tag{42}$$

where h is the average edge length for the grid, q is the order of the truncation error, and C is the convergence-rate constant. To estimate q we evaluated the error on a sequence of grids. Using the error estimate on two grids, h and h', the order of the truncation error can be estimated.

$$q \approx \frac{\log_{10} \frac{||E_h||}{||E_{h'}||}}{\log_{10} \frac{h}{h'}} \tag{43}$$

In our numerical experiments we used the discrete L_2 norm.

The two divergence operators produce a vector defined at the grid points. The L_2 norm used to measure this truncation error is

$$||E_{L_2}|| = \left[\sum_p (\mathbf{e}_p, \mathbf{e}_p) V_p \right]^{\frac{1}{2}}, \tag{44}$$

where $\mathbf{e}_p = (\mathbf{DIV}\ \mathbf{T})_p - (\nabla \cdot \mathbf{T})_p$. $(\mathbf{DIV}\ \mathbf{T})_p$ is the result from the discrete operator, $(\nabla \cdot \mathbf{T})_p$ is the exact solution evaluated at point p, and V_p is the volume of the point.

For the two gradient operators, where the result is a tensor held as edge or median mesh projections, the norm we use is

$$||E_{L_2}|| = \left[\sum_z (\mathbf{E}_z, \mathbf{E}_z) V_z\right]^{\frac{1}{2}}. \tag{45}$$

To evaluate the tensor scalar product in a zone equation (28) or (37) is used as appropriate. The edge projections of error tensor $\mathbf{E}$ are

$$\mathbf{E}^e_{p+\frac{1}{2}} = \mathbf{G}^e_{p+\frac{1}{2}} - (\nabla \mathbf{v})^e_{p+\frac{1}{2}} \cdot \hat{\mathbf{e}}^e_{p+\frac{1}{2}}, \tag{46}$$

and the median mesh projections are

$$\mathbf{E}^z_p = \mathbf{G}^z_p - (\nabla \mathbf{v})^z_p \cdot \hat{\mathbf{s}}^z_p. \tag{47}$$

The exact solution is evaluated using the coordinate of the center point of the zone edge or median mesh segment. In our numerical experiments, we ignore the errors at the points and zones on the boundary.

Table 1 shows values of q for **GRAD v**, calculated as normal projections to the median mesh. The table does not contain results for the combinations of grid and function where the truncation error is zero. The results show that the operator has approximately first-order convergence on all grids where truncation error is present.

Table 2 shows values of q for **DIV T**, when $\mathbf{T}$ is defined as the tangential projections on the zone edges. Again only results for the combinations where truncation error was present are shown. The table shows that for the transformed grids with the triangular and quadrilateral zones the operator has approximately second-order convergence, while for the grids with hexagonal zones it only has first-order convergence. Also the error norm is larger for the hexagonal grids. The quadrilateral grid is logically rectangular, and the triangular grid can be constructed by taking a logically rectangular grid and splitting each zone in half. Thus, although both triangular and quadrilateral grids are structured, the hexagonal grid is not. This difference may be the underlying cause for the reduced order of convergence.

The truncation errors for the prime operator **DIV T** shown in table 3 are for $\mathbf{T}$ defined as the normal projection of the tensor to the median mesh. As for the derived divergence it shows second-order convergence for the grids with quadrilateral and triangular zones, and first-order for the grid with hexagonal zones. The errors are smaller than for the derived divergence. The results show that the convergence rate for the smooth hex mesh is higher than for the regular hex mesh, however both sets are going to first order, and the magnitude of the error on the smooth mesh is larger.

The prime operator, **GRAD v** calculated as the tangential projection to the zone edges, gave results exact to round-off error for all twelve combinations of grids and functions in this test.

Grid	Function	h	L_2 norm	q_{L2}
Smooth Tri	Quadratic	0.05126	0.01223	0.77
		0.02566	0.00719	0.90
		0.01284	0.00385	0.95
		0.00642	0.00198	0.98
		0.00321	0.00101	-
Smooth Quad	Linear	0.05291	0.04036	0.83
		0.02643	0.02268	0.92
		0.01321	0.01197	0.96
		0.00660	0.00614	0.98
		0.00330	0.00311	-
Smooth Quad	Quadratic	0.05291	0.12662	0.80
		0.02643	0.07274	0.91
		0.01321	0.03880	0.95
		0.00660	0.02001	0.98
		0.00330	0.01016	-
Regular Hex	Quadratic	0.04811	0.00884	0.88
		0.02406	0.00481	0.98
		0.01203	0.00243	0.98
		0.00601	0.00123	0.98
		0.00301	0.00062	-
Smooth Hex	Linear	0.04968	0.01413	0.76
		0.02512	0.00842	0.98
		0.01262	0.00428	0.96
		0.00633	0.00220	0.99
		0.00317	0.00111	-
Smooth Hex	Quadratic	0.04968	0.04207	0.76
		0.02512	0.02498	0.96
		0.01262	0.01294	0.97
		0.00633	0.00661	0.98
		0.00317	0.00334	-

Table 1: Truncation error for the derived operator **GRAD v**, defined by Eqn. (39). The error is for the normal projection of the tensor to the median mesh.

Grid	Function	h	L_2 norm	q_{L2}
Smooth Tri	Linear	0.05126	0.01107	1.89
		0.02566	0.00299	1.96
		0.01284	0.00077	1.99
		0.00642	0.00019	1.99
		0.00321	0.00005	-
Smooth Tri	Quadratic	0.05126	0.03031	1.88
		0.02566	0.00824	1.96
		0.01284	0.00212	1.98
		0.00642	0.00054	1.99
		0.00321	0.00014	-
Smooth Quad	Linear	0.05291	0.04053	1.84
		0.02643	0.01127	1.95
		0.01321	0.00292	1.98
		0.00660	0.00074	1.99
		0.00330	0.00019	-
Smooth Quad	Quadratic	0.05291	0.14377	1.87
		0.02643	0.03923	1.95
		0.01321	0.01011	1.98
		0.00660	0.00256	1.99
		0.00330	0.00064	-
Regular Hex	Quadratic	0.04811	0.02285	0.86
		0.02406	0.01257	0.94
		0.01203	0.00657	0.97
		0.00601	0.00336	0.98
		0.00301	0.00170	-
Smooth Hex	Linear	0.04968	0.51097	0.93
		0.02512	0.27094	0.97
		0.01262	0.13912	0.98
		0.00633	0.07045	0.99
		0.00317	0.03544	-
Smooth Hex	Quadratic	0.04968	0.59806	0.98
		0.02512	0.30638	0.97
		0.01262	0.15684	0.98
		0.00633	0.07979	0.99
		0.00317	0.04031	-

Table 2: Truncation error for the derived operator **DIV T**, defined by Eqn. (33). The truncation error is second-order of the triangular and quadrilateral grids, but first-order on the unstructured hexagonal grids.

Grid	Function	h	L_2 norm	q_{L2}
Smooth Tri	Quadratic	0.05126	0.00770	1.94
		0.02566	0.00201	1.97
		0.01284	0.00051	1.99
		0.00642	0.00013	1.99
		0.00321	0.00003	-
Smooth Quad	Quadratic	0.05291	0.01561	1.98
		0.02643	0.00396	1.99
		0.01321	0.00099	2.00
		0.00660	0.00025	2.00
		0.00330	0.00006	-
Regular Hex	Quadratic	0.04811	0.00286	0.86
		0.02406	0.00157	0.94
		0.01203	0.00082	0.97
		0.00601	0.00042	0.98
		0.00301	0.00021	-
Smooth Hex	Quadratic	0.04968	0.01813	1.66
		0.02512	0.00583	1.53
		0.01262	0.00204	1.25
		0.00633	0.00086	1.07
		0.00317	0.00041	-

Table 3: Truncation error for the prime operator **DIV T**, defined by Eqn. (35). Here **T** is defined as the normal projection of the tensor to the median mesh. As in table 2 the truncation error is second-order on the structured grids and first order on the unstructured hexagonal grids. Note that the error are much smaller than for the derived divergence results in Table 2.

4.2 Numerical solution of a vector Poisson equation

To test the operators we have used them to solve the problem

$$\nabla \cdot (\nabla \mathbf{u}) = \mathbf{f}, \tag{48}$$

$$\mathbf{f} = \begin{pmatrix} -2 \ \sin x \ \cos y \\ -2 \ \sin x \ \cos y \end{pmatrix}, \tag{49}$$

with Dirichlet boundary conditions. The exact solution for this problem is

$$\mathbf{u} = \begin{pmatrix} \sin x \ \cos y \\ \sin x \ \cos y \end{pmatrix}, \tag{50}$$

$\mathbf{u}$ is defined on the boundary.

In addition to the L_2 norm used for the truncation error tests, the max norm was also calculated. This norm is

$$||E_{\max}|| = \max_{1 \le i \le N_p} |e_{x,i}, e_{y,i}|, \tag{51}$$

where e_x and e_y are the components of the error vector

$$\mathbf{e}_p = (\textbf{DIV GRAD } \mathbf{u}_p) - (\nabla \cdot \nabla \mathbf{u})_p. \tag{52}$$

Tables 4 and 5 show the convergence rates for the solution of (48) for the discrete approximations where the tensor solution is defined as either the tangential projection or normal projection operators. Both sets of results show similar behavior for all the grids. On the triangular and quadrilateral grids both the L_2 and max norms show approximately second order convergence. On the hexagonal grids the max norm has approximately first order convergence, and the L_2 norm gives between first and second order convergence.

5 Conclusion

We have constructed two sets of discrete expressions for the gradient of a vector and divergence of a tensor on unstructured grids. The first set of discrete operators are appropriate when tensor functions are defined as the tangential projections to the zone edges. The second set of operators are appropriate when the tensor functions are defined as normal projections to the median mesh. Both sets have vector functions defined at the grid points. These mimetic finite difference methods were defined using the support operator method. Each set of operators can be combined to give an expression for the vector Laplacian.

The order of accuracy of the truncation error was investigated on triangular, quadrilateral and hexagonal grids. The truncation error converged between first and second-order. When tensors are defined as tangential projections, the gradient operator was exact for quadratic polynomials. The derived divergence gave second-order truncation error on grids with triangular and quadrilateral zones, and was first-order for the grids with hexagonal zones. When the tensors

Grid	h	L_2 norm	q_{L2}	Max norm	$q_{\max}$
Regular	0.0500000	0.0000040	2.00	0.0000081	2.00
Tri	0.0250000	0.0000010	2.00	0.0000020	2.00
	0.0125000	0.0000002	2.00	0.0000005	2.00
	0.0062500	0.0000001	-	0.0000001	-
Smooth	0.0493239	0.0000334	2.06	0.0000994	2.03
Tri	0.0252017	0.0000084	2.03	0.0000255	2.02
	0.0127241	0.0000021	2.01	0.0000064	2.01
	0.0063913	0.0000005	-	0.0000016	-
Regular	0.0500000	0.0000099	2.00	0.0000132	2.00
Quad	0.0250000	0.0000025	2.00	0.0000033	2.00
	0.0125000	0.0000006	2.00	0.0000008	2.00
	0.0062500	0.0000002	-	0.0000002	-
Smooth	0.0525892	0.0002774	1.95	0.0005161	1.91
Quad	0.0263507	0.0000721	1.99	0.0001382	1.98
	0.0131877	0.0000182	2.00	0.0000350	2.00
	0.0065966	0.0000046	-	0.0000088	-
Regular	0.0481125	0.0005288	1.36	0.0019595	0.94
Hex	0.0240563	0.0002067	1.31	0.0010245	0.98
	0.0120281	0.0000834	1.22	0.0005204	0.98
	0.0060141	0.0000357	-	0.0002629	-
Smooth	0.0504807	0.0009455	1.57	0.0025585	0.94
Hex	0.0253050	0.0003195	1.55	0.0013334	0.99
	0.0126666	0.0001095	1.41	0.0006706	1.00
	0.0063365	0.0000413	-	0.0003363	-

Table 4: The errors and convergence rates for solving Poisson's equation when the gradient is the prime operator, and the tensors are defined as tangential projections to the zone edges.

Grid	h	L_2 norm	q_{L2}	Max norm	$q_{\max}$
Regular	0.0500000	0.0000040	2.00	0.0000081	2.00
Tri	0.0250000	0.0000010	2.00	0.0000020	2.00
	0.0125000	0.0000002	2.00	0.0000005	2.00
	0.0062500	0.0000001	-	0.0000001	-
Smooth	0.0493239	0.0000334	2.06	0.0000994	2.03
Tri	0.0252017	0.0000084	2.03	0.0000255	2.02
	0.0127241	0.0000021	2.01	0.0000064	2.01
	0.0063913	0.0000005	-	0.0000016	-
Regular	0.0500000	0.0000099	2.00	0.0000132	2.00
Quad	0.0250000	0.0000025	2.00	0.0000033	2.00
	0.0125000	0.0000006	2.00	0.0000008	2.00
	0.0062500	0.0000002	-	0.0000002	-
Smooth	0.0525892	0.0009477	1.99	0.0018962	1.98
Quad	0.0263507	0.0002397	2.00	0.0004816	1.99
	0.0131877	0.0000601	2.00	0.0001211	2.00
	0.0065966	0.0000150	-	0.0000303	-
Regular	0.0481125	0.0007079	1.70	0.0038118	1.02
Hex	0.0240563	0.0002181	1.60	0.0018793	1.01
	0.0120281	0.0000717	1.51	0.0009323	1.01
	0.0060141	0.0000252	-	0.0004642	-
Smooth	0.0504807	0.0009534	1.60	0.0036081	0.71
Hex	0.0253050	0.0003167	1.55	0.0022146	0.92
	0.0126666	0.0001080	1.50	0.0011717	0.98
	0.0063365	0.0000382	-	0.0005946	-

Table 5: The errors and convergence rates for solving Poisson's equation when the divergence is the prime operator, and the tensors are defined as normal projections to median mesh.

are defined as normal projections, the divergence was second-order accurate for the deformed triangular and quadrilateral grids, and first-order on the deformed hexagonal grid. The truncation error for the derived gradient converged to first order on all grids considered. In both cases the magnitude of the error of the prime operator is less than the magnitude for the equivalent derived operator.

The solution of the Poisson equation converged to second-order for both approximations of the Laplacian on the triangular and quadrilateral grids. On the hexagonal grids the solution converged between first and second-order.

The new discrete operators are suitable for the solution of partial differential equations on arbitrary two dimensional grids. The numerical experiments show that the operators have good truncation error and convergence properties, with convergence rate of between first and second order. The truncation error tests show that the prime operators have a smaller error magnitude than the derived operator. This affects which approximation is most suitable for a specific problem, if the accuracy of one operator is more critical then that operator should be chosen as prime operator.

Acknowledgements
This research is supported by the Department of Energy, under contract W-7405-ENG-36.

References

[1] J.M. Hyman and M. Shashkov. Natural discretizations for the divergence, gradient and curl on logically rectangular grids. *Computers Math. Applic.* **33**, 81–104, (1997).

[2] J.M. Hyman and M. Shashkov. Adjoint operators for the natural discretizations of the divergence, gradient and curl on logically rectangular grids. *IMACS J. Appl. Numer. Math.* **25**, 413–442, (1997).

[3] J.M. Hyman and M. Shashkov. Approximations of boundary conditions for mimetic finite-difference methods. *Computers Math. Applic.* **36**, 79–99, (1998).

[4] M. Shashkov and S. Steinberg. Solving diffusion equations with rough coefficients in rough grids. *J. Comput. Phys.* **129**, 383–405, (1996).